Kovove Mater. 63 2025 299–308
DOI: 10.31577/km.2025.5-6.299

Evaluation of microstructure, martensite morphology, and tensile properties of API X60 dual-phase pipeline steel

Abdelkader Djilali Hammou[1], Zidelmel Sami[1], Kaouka Alaeddine[2]

[1] *Process Engineering Laboratory, Amar Telidji University, 03000 Laghouat, Algeria*
[2] *Laboratory of Applied Sciences and Didactics, Higher Normal School of Laghouat, 03000 Laghouat, Algeria*

Received 17 October 2025, received in revised form 14 November 2025, accepted 5 December 2025

Abstract

This study evaluated the microstructure, martensite morphology, and mechanical properties of API X60 dual-phase pipeline steel, aiming to understand the relationship between microstructure and mechanical properties. Following annealing at various intercritical temperatures (740, 760, 780, and 810 ℃), X60 dual-phase steel with varying martensite volume fractions was produced. To create distinct martensite morphologies, three treatments were developed. Due to the Intermediate Quenching (IQ) treatment, fine and fibrous martensite morphology was formed, which was evenly distributed throughout the ferrite matrix. The Direct Quenching (DQ) treatment showed dispersed martensite islands within a ferritic matrix. However, the martensite and ferrite morphologies produced by the Step Quenching (SQ) treatment were blocky and banded. Results revealed that increasing the amount of martensite improves both yield strength and ultimate tensile strength while decreasing ductility. This result indicated that adjusting heat treatment parameters can optimize X60 (DP) steel for strength-critical applications. According to the results of the experiment, API X60 (DP) steel with a finely distributed microstructure has higher tensile strength than steel with other microstructures.

K e y w o r d s: microstructure, mechanical properties, intercritical annealing temperature, X60 dual-phase steel, work hardening, tensile strength

1. Introduction

Dual-phase (DP) steels are a class of high-strength low-alloy steels that have attracted significant attention in the automotive and structural pipeline industries due to their unique combination of high strength and favorable formability [1, 2]. Their microstructure typically consists of a hard martensite phase dispersed within a soft ferrite matrix [3]. It is this dual-phase (DP) structure that confers steels their advantageous mechanical properties. (DP) steels are often produced through a controlled annealing process involving intercritical annealing, in which the steel is heated to a temperature between the lower (Ac_1) and upper (Ac_3) critical temperatures, then rapidly cooled. This process leads to the partial conversion of austenite to martensite, resulting in the desired (DP) microstructure [4]. (DP) steels are used in various structural components to enhance safety and fuel efficiency. They are also suitable for pipeline applications, offering the combination of deformability, high strength, and toughness required for transporting crude oil and gas in severe conditions [5, 6]. Studies show that increasing the intercritical annealing temperature generally increases the martensite volume fraction. For instance, according to Zhou et al. [7], the martensite volume fraction increased from 10.29 to 61.22 % as the intercritical temperature increased from 730 to 850 ℃. Similarly, Hao et al. [8] reported an increase in the martensite volume fraction from 53 to 71 % when the temperature was raised from 750 to 850 ℃. The mechanical characteristics of DP steels are influenced by martensite morphology, which varies with the heat treatment used, including Direct Quenching (DQ), Step Quenching (SQ), and Intermediate Quenching (IQ). These treatments produce different martensite

*Corresponding author: e-mail address: a.kaouka@lagh-univ.dz

Table 1. X60 steel's chemical composition (wt.%)

Elements	C	Mn	Si	S	P	Nb	V	Ti	Al
API X 60	0.10	1.30	0.25	0.001	0.011	0.035	0.04	0.002	0.032

morphologies, including fine, fibrous, blocky, banded, and island types, each of which affects tensile properties differently [9]. The selection of (IQ), (DQ), and (SQ) in (DP) steel heat treatments is based on their ability to tailor the microstructure, particularly the martensite morphology and distribution, which directly affects mechanical properties. IQ treatment involves quenching to produce a fine-fibrous martensite-ferrite mixture evenly dispersed. This produces a finely distributed martensite microstructure associated with higher tensile strength and good toughness. It usually starts with full austenitizing, water quenching to martensite, followed by intercritical annealing to adjust phase fractions. DQ treatment creates dispersed martensite islands in a ferritic matrix via direct quenching from the intercritical range. This method aims to balance strength and ductility by controlling martensite volume and morphology. SQ treatment involves full austenitizing, intercritical annealing, and final quenching. This process can produce blocky, banded microstructures and is valued for reducing the number of heat-treatment steps, improving production efficiency while allowing control over ferrite and martensite fractions. It is often used to develop advanced microstructures with tailored mechanical behavior and better processing control. The morphology of martensite significantly influences the tensile strength of (DP) steel by affecting the interaction between the hard martensite phase and the soft ferrite matrix. Finer and more uniformly distributed martensite structures enhance tensile strength more effectively by improving strain distribution and work hardening. Distributed fine martensite enhances stress transfer to the ferrite and delays strain localization, thereby improving tensile strength and ductility [10, 11]. The mechanical properties of (DP) steel, such as tensile strength, yield strength, and ductility, are highly dependent on the intercritical annealing temperature [12]. Generally, increasing the intercritical temperature increases tensile strength due to a higher martensite volume fraction. However, this effect often comes at the expense of ductility [13]. This trade-off between strength and ductility necessitates careful selection of the intercritical temperature to optimize the overall performance of the X60 (DP) steel. According to the literature, few studies focus on the (DP) structure of X60 pipeline steels by varying the morphology and volume fraction of martensite. The primary purpose of X60 (DP) steel research is to develop and understand steels that combine high strength with excellent formability, thereby meeting the demands of industrial applications, particularly in the hydrocarbon sector. This research aims to optimize the microstructure, typically a ferrite matrix with dispersed islands of martensite, to achieve a superior balance of mechanical properties, including strength and ductility.

2. Experimental methodology

Table 1 delineates the chemical composition of the X60 pipeline steel examined in this study. Alpha Pipe Gas Society supplied the steel in Ghardaia, Algeria. The amounts of Phosphorus (P) and Sulfur (S) impurities are rather low, particularly sulfur.

We use three kinds of heat treatment to create different morphologies of (DP) steels. The (IQ) treatment consisted of two treatments. After 30 minutes of soaking at 950 ℃, the samples were water-cooled. They were then maintained at intercritical temperatures of 740, 760, 780, and 810 ℃ for 30 minutes, after which they were soaked in water. For (DQ) treatment, the samples are heated directly to the intercritical temperatures (740, 760, 780, and 810 ℃) for 30 minutes, then quenched in water. In the (SQ) treatment, the samples were initially soaked at 950 ℃ for 30 minutes. After that, they were cooled to the Intercritical Annealing Temperature (IAT) of 740, 760, 780, or 810 ℃ in a furnace. The specimens were held at this temperature for 30 minutes, then water quenched. For metallographic analysis, specimens from various treatments were sliced and mounted. We etched the specimens using a 3% nital solution and then conventional grinding and polishing methods. The entire microstructure of API X60 pipeline steel was compared using a Scanning Electron Microscope (SEM) and conventional light microscopy. To calculate the martensite and ferrite volume fractions, a manual point-counting technique was employed. At room temperature, the tensile strength of the flat specimens was assessed using a computer-controlled Mohr Federhaff Lasenhausen system machine. This analysis was conducted in accordance with ASTM A370. The Tescan Vega3 Scanning Electron Microscope (SEM) was used to examine the fracture surfaces of the tensile specimens.

3. Results and discussion

3.1. Microstructural analysis of API X60 pipeline steel

Figure 1 presents a SEM micrograph of the specimen's microstructure, consisting of ferrite and pearlite

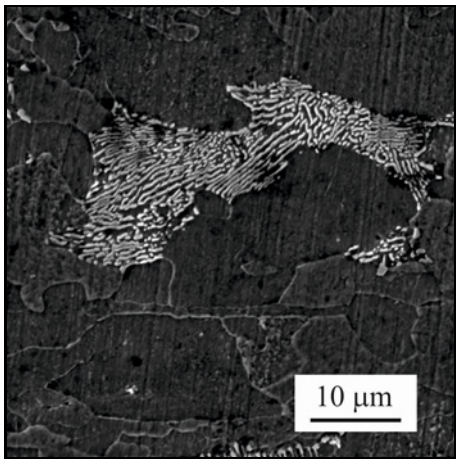

Fig. 1. Ferrite-pearlite microstructure of as-received X60 steel.

phases. The ferrite matrix appears as the dark region, while the pearlite is the lighter area, primarily located at grain boundaries. The pearlite lamellae are clearly visible near the ferrite matrix. Using the reverse segment method, the pearlite concentration in X60 steel was determined to be approximately 13 %.

3.2. Development of DP structure

(DP) steel develops through controlled heat treatment, starting with a ferrite-pearlite microstructure. The steel is heated to an intercritical temperature, where both ferrite and austenite coexist, allowing austenite to form from regions enriched in carbon, whether from pearlite or ferrite. Upon rapid quenching, the austenite transforms into martensite, forming a dual-phase microstructure composed of soft ferrite and hard martensite islands. This combination provides a balance of high strength and good ductility, with the martensite strengthening the steel and ferrite contributing to its formability. Process parameters, such as temperature, heating time, and cooling rate, significantly influence the fraction and morphology of martensite and ferrite, thereby tailoring the steel's mechanical properties. This microstructure is widely used for its excellent strength and formability in automotive and structural applications.

3.2.1. Effect of Intercritical Annealing Temperature (IAT) on Martensite Volume Fraction (MVF)

The optical micrographs of the X60 samples undergoing (SQ) heat treatment at various critical annealing temperatures are revealed in Fig. 2. It is crucial to know the Intercritical Annealing Temperature (IAT) for determining the Martensite Volume Fraction (MVF) in (DP) steels. The microstructure of (DP)

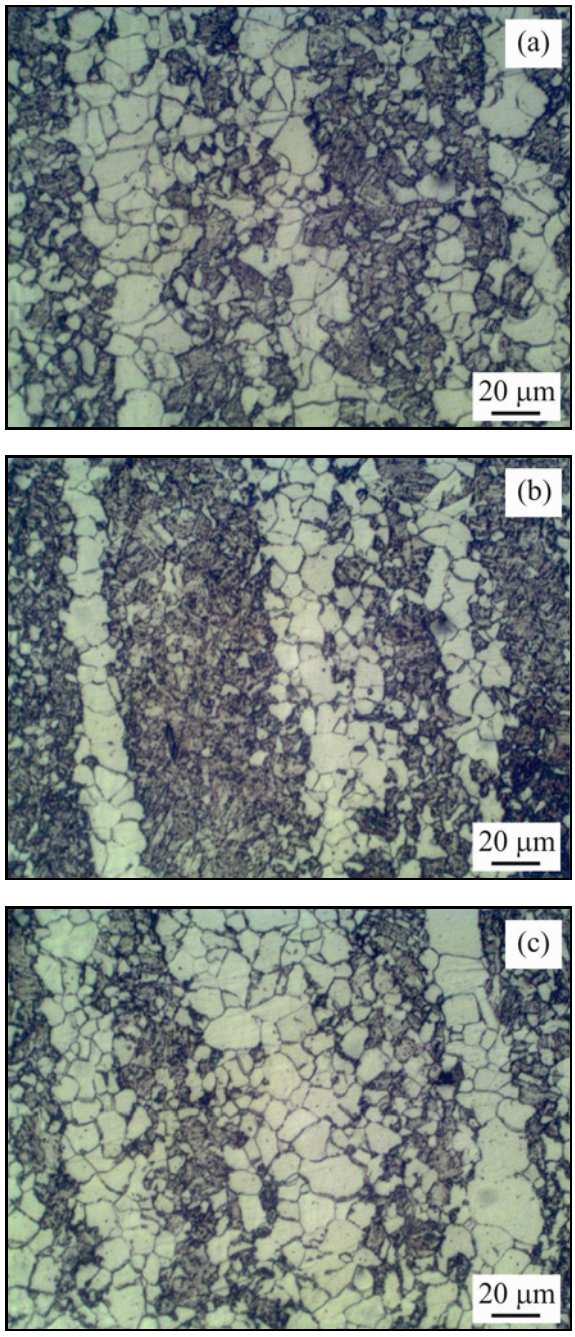

Fig. 2. Optical micrographs of dual-phase X60 steel after (SQ) treatment at different intercritical annealing temperatures X500: (a) 740 °C, (b) 780 °C, and (c) 810 °C.

steels are defined by a hard martensite phase and a soft ferrite matrix. Increasing the (IAT) in X60 (DP) steel results in a higher volume fraction of martensite after subsequent quenching. At lower (IAT), 740 °C, only a small amount of austenite is formed, resulting in lower martensite content after quenching. A higher (IAT), 810 °C, leads to more martensite formation in X60 steel primarily because increasing the temperature within the intercritical region (between

Table 2. The relationship between the MVF and the IAT

	Intercritical annealing temperatures (℃)			
	740	760	780	810
MVF (%)	21	34	52	57

Ac_1 and Ac_3) promotes the transformation of more phases into austenite during annealing [16]. Upon subsequent rapid cooling (quenching), this larger fraction of austenite transforms into martensite, resulting in a higher volume fraction of martensite in the final (DP) microstructure.

For example, increasing the (IAT) from 740 to 810 ℃ has been shown to enhance the martensite phase fraction from 21 to 57 %, as shown in Table 2. The intercritical annealing temperature affects the martensite volume fraction, rather than the specific intercritical heat treatments used. Shi et al. and Ahmed et al. [17, 18] reported that, at the same intercritical annealing temperature, the martensite volume fraction was identical across different intercritical heat treatments.

3.2.2. Effect of annealing treatment schedule on martensite morphologies

Scanning electron micrographs of X60 steel after three distinct heat treatments (DQ), (SQ), and (IQ) are seen in Fig. 3. All heat treatments exhibit dual-phase ferrite-martensite microstructures. However, the type of heat treatment significantly affects the shape of the martensitic phase [19]. The observed disparities in martensite form and distribution can be explained by variations in the initial microstructural condition of the X52 samples before entering the intercritical domain ($\alpha + \gamma$) [20, 21]. Figure 3a shows a (DP) microstructure developed from an initial ferrite-pearlite microstructure (DQ treatment). This process involves heating the steel to a temperature at which both ferrite and austenite coexist, then quenching. This treatment allows conversion of austenite to martensite upon cooling, resulting in a microstructure typically consisting of dispersed martensite islands within a ferritic matrix.

Figure 3b shows the microstructure (ferrite + martensite) of X52 steel that has experienced (SQ) treatment. This microstructure has a banded morphology with a non-uniform distribution of phases. In the biphasic domain for (SQ) treatment, the austenite phase appears first before annealing. During slow cooling, ferrite preferentially nucleates at the austenitic grain boundaries located in manganese-poor areas. Austenitizing temperatures influence the dissolution

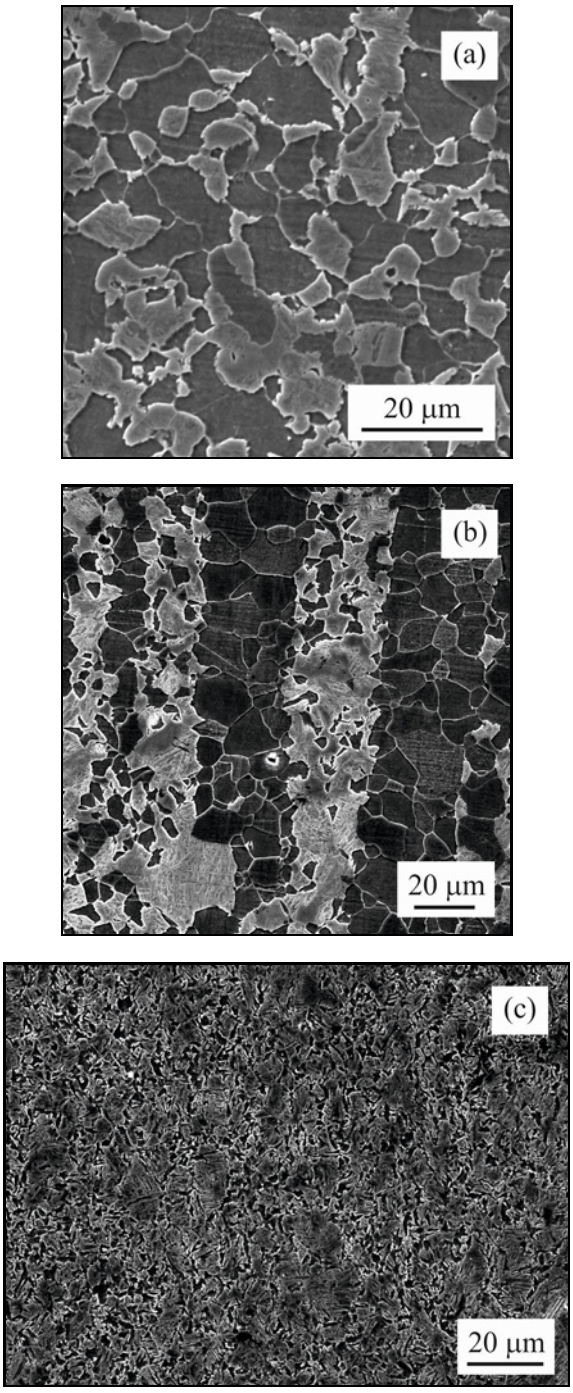

Fig. 3. SEM Micrographs of dual-phase X60 steel at 780 ℃ for different heat treatments: (a) DQ treatment, (b) SQ treatment, and (c) IQ treatment.

of pearlite bands and the homogenization of carbon distribution in banded dual-phase steels. It concludes that higher austenitizing temperatures reduce banding intensity and promote a more uniform ferrite-martensite structure, thereby improving mechanical consistency across the material [22]. The areas of untransformed austenite change into martensite after

quenching, but the arrangement remains the same. After quenching from the ($\alpha+\gamma$) domain, this results in a (DP) microstructure with alternating bands of ferrite and martensite. A (DP) microstructure, achieved after treatment (IQ), is depicted in Fig. 3c. The interaction between ferrite and martensite during deformation is characterized by strain partitioning, where ferrite accommodates early deformation and hardens near martensite interfaces, while martensite work hardens and plastically deforms, contributing to strength and ductility. It is defined by a microstructure comprising fine, fibrous martensite evenly distributed within a ductile ferrite matrix. During heating to intercritical temperatures ($\alpha+\gamma$), austenite nucleates from the initial fully martensitic microstructure at the joints of the previous austenite grains and the joints of martensite laths. This results in acicular areas that, upon room-temperature quenching, transform into fine martensite particles. A homogeneous distribution of nucleation sites facilitates the development of martensite with fine grain size and morphology.

3.3. The tensile properties in relation to the Intercritical Annealing Temperature (IAT)

Figure 4 shows the variation in conventional yield strength (YS) and tensile strength (TS) as a function of intercritical temperature for X60 steel. These curves show the general trend that the strength of (DP) steels increases with intercritical temperature, or the growth in the volume fraction of martensite, for a given heat treatment. Increasing (MVF) raises the yield and tensile strengths markedly. This is because martensite is a harder phase than ferrite; consequently, steel's strength is increased by a larger volume proportion of martensite [21]. The tensile strength is usually directly related to the amount of martensite in the microstructure [22, 23]. As the martensite volume fraction (MVF) increases, both the yield and tensile strengths increase markedly. This is because martensite is a hard phase that strengthens the steel matrix. The tensile strength often shows a near-linear increase with martensite content. Increased (MVF) leads to a higher dislocation density near ferrite-martensite interfaces due to the volumetric expansion of martensite during transformation. This interface strengthening contributes to higher yield and tensile strengths.

The ductility of (DP) steels was studied in terms of total elongation. The variation in elongation of (DP) structures as the intercritical temperature changes of X60 steel is exposed in Fig. 4. In general, the elongation of X60 (DP) steel decreases as the intercritical temperature increases. This is due to an increase in the volume fraction of hard, brittle martensite. On the other hand, as the Martensite Volume Fraction (MVF) increases, ductility decreases because the brittle nature of martensite makes the steel stiffer and less

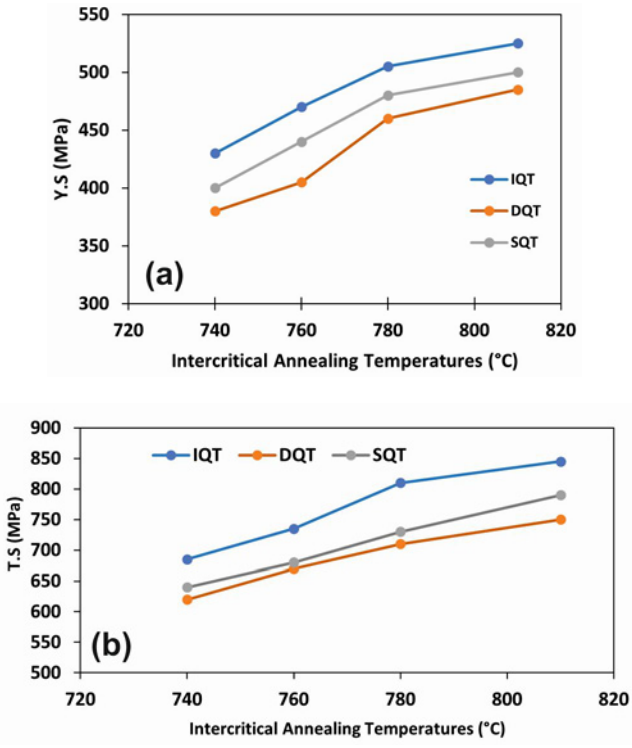

Fig. 4. Tensile properties as a function of intercritical annealing temperatures.

able to undergo plastic deformation. Additionally, the morphology of the martensite plays a key role in ductility: fine, evenly distributed martensite tends to enhance formability compared to coarse, blocky martensite structures at similar (MVF) levels. This fine fibrous martensite improves the steel's ability to deform without fracturing. Therefore, both the amount and the distribution of martensite significantly influence the mechanical behavior of (DP) steels. The morphology of martensite determines the ductility of (DP) steels, with fine structures exhibiting better ductility. X60 steel that has undergone (SQ) treatment has the lowest elongation at break compared to steel that has undergone (IQ) and (DQ) heat treatments. The ferrite grains breaking brittlely before the martensite cracks during necking are probably the cause of the poor elongation value for the (SQ) treatment. This results from the local internal stress generated during deformation near the ferrite/martensite interface. The banded microstructure leads to more severe heterogeneous deformation of the ferritic matrix. Finely distributed, fibrous martensite morphology is generally more beneficial for mechanical performance because it enables better load transfer and delays strain localization. Coarser or banded martensite morphologies promote uneven strain distribution, causing premature failure. The morphology influences dislocation generation, strain partitioning between phases, and work-

Table 3. Tensile properties of X60 steel as a function of IAT

		Intercritical annealing temperatures (°C)			
		740	760	780	810
Yield strength YS (MPa)	SQ	400	440	480	500
	IQ	430	470	505	525
	DQ	380	405	460	485
Tensile strength TS (MPa)	SQ	580	680	730	790
	IQ	685	735	810	845
	DQ	640	670	710	750
Total elongation A (%)	SQ	20	16	13	11
	IQ	34	31	27	25
	DQ	26	22	20	16.5

hardening capacity, all of which govern the balance of strength and ductility in (DP) steel. Studies in the literature have shown that in (DP) steels, the mismatch in mechanical properties between the ductile ferrite and the harder martensite leads to strain incompatibilities during plastic deformation, resulting in stress concentration at phase boundaries [22–26]. This phenomenon is particularly pronounced in microstructures with coarse or banded ferrite grains, which promote heterogeneous deformation. The banded microstructure, in particular, exacerbates heterogeneity, leading to more severe internal stresses within the ferritic matrix. Such heterogeneity has been reported to facilitate early crack initiation in ferrite, which acts as the crack nucleation site and limits tensile elongation. Furthermore, the accumulation of internal stress near the ferrite/martensite interface during deformation increases the likelihood of brittle fracture in ferrite. This is supported by microscopic observations indicating that brittle failure in ferrite occurs prior to martensite cracking in microstructures with insufficient phase uniformity. The large disparity in mechanical strength and elongation between phases drives this initial failure, which then propagates through the ferrite matrix, impacting overall ductility. In contrast, microstructures with fine, well-dispersed martensite, such as those obtained through specific heat treatments, tend to distribute internal stress more evenly, thereby delaying or suppressing brittle ferrite failure. This aligns with findings that microstructural refinement and homogeneous phase distribution improve ductility by reducing stress concentration and crack initiation sites within the ferritic phase. Hence, the microstructural features influence the failure mechanism in dual-phase steels. The literature supports the idea that the combination of phase heterogeneity, microstructural banding, and the resulting local stress concentration is a primary driver of the brittle failure of ferrite grains before martensite, thereby impacting tensile elongation performance.

Increasing the martensite volume fraction typically reduces elongation, indicating a decrease in ductility. This happens because the harder martensite phase limits the steel's overall plastic deformation capacity. Table 3 summarizes the specimens' conventional yield strength, tensile strength, and elongation at break after (IQ), (DQ), and (SQ) treatments. The kind of heat treatment has a substantial impact on the tensile characteristics. Differences in morphology and the volume fraction of the martensitic phase are responsible for this variation.

A comparison of the mechanical properties between the (IQ), (DQ), and (SQ) samples reveals that the (IQ) sample exhibits significantly higher values for the yield strength, tensile strength, and total elongation. This observation is in excellent agreement with the reports of Bayram et al. [27] and Bag et al. [28]. Compared with (DQ) and (SQ) treatments, these mechanical characteristics indicate that the fine, fibrous martensite generated by the (IQ) treatment has the best strength-to-ductility ratio, regardless of the intercritical temperature.

3.4. Work hardening phenomenon

(DP) steels exhibit high work-hardening capacity, a phenomenon in which metals strengthen during plastic deformation, which is closely linked to their microstructure, particularly the volume fraction, morphology, and distribution of the martensite phase within the ferrite matrix [32]. The strain-hardening coefficient (n) is a key indicator of this behaviour. Higher values of (n) allow for greater deformation before necking occurs. The following Hollomon equation can describe the flow behavior of most metals and alloys:

$$\sigma = K\varepsilon^n, \tag{1}$$

where K and n are constants called the stress coef-

Table 4. Work-hardening coefficients for X60 steel at different IAT

Work-hardening coefficient		Intercritical annealing temperatures (°C)			
		740	760	780	810
IQ	n_1	0.36	0.38	0.40	0.41
	n_2	0.12	0.13	0.14	0.14
DQ	n_1	0.39	0.42	0.44	0.45
	n_2	0.14	0.15	0.17	0.18
SQ	n_1	0.42	0.44	0.46	0.47
	n_2	0.16	0.18	0.19	0.20

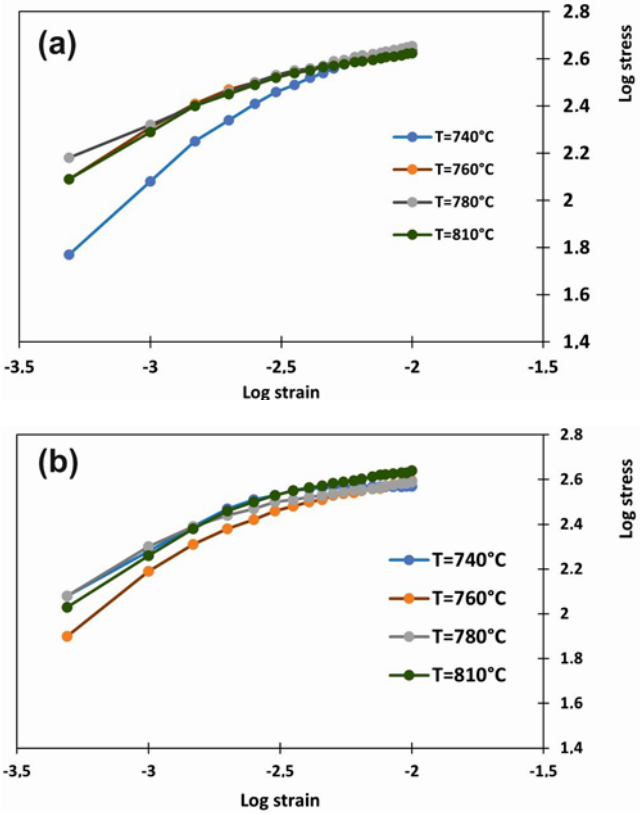

Fig. 5. Variation of the strain hardening coefficient as a function of intercritical annealing temperatures: (a) DQ treatment and (b) IQ treatment.

ficient and strain hardening coefficient, respectively. The variation of $\log(\sigma)$ as a function of $\log(\varepsilon)$ for X60 steel subjected to different heat treatments is illustrated in Fig. 5. This non-linear variation indicates that the work hardening phenomenon of this X60 (DP) steel obeys the two-stage work hardening mechanism [35]. The changes in the work-hardening coefficients (n_1) and (n_2) for the two work-hardening stages as the intercritical temperature changes are shown in Table 4. As shown in this table, both coefficients increase with increasing (ICT). For all microstructures, the work hardening coefficient of the first stage (n_1) is higher than that of the second stage (n_2). The work-hardening exponent (n) in (DP) steels exhibits two stages, one related to ferrite and the other to ferrite-martensite plastic deformation. Initially, ferrite deforms plastically, while martensite deforms elastically at low plastic deformation levels, with the work-hardening coefficient (n_1) dependent on the martensite volume fraction. Increased ferrite stress correlates with higher mobile dislocation density near martensite islands, driven by higher critical annealing temperature (IAT). Research indicates that the work hardening in (DP) steel is affected by the microstructure, with an increased volume fraction of martensite (MVF) correlating with a higher work hardening coefficient (n) [33, 34]. The martensite phase morphology significantly influences work hardening; finer, uniformly distributed martensite enhances stress transfer between phases, thereby improving energy absorption during deformation [37]. Variations in martensite types, such as fibrous morphologies, lead to higher strain-hardening rates, which are crucial for applications requiring toughness and deformation resistance.

4. Modes of failure during a tensile test

The tensile fracture properties of (IQ) specimens composed of X60 (DP) steel are shown in Fig. 6, which illustrates the impact of different intercritical annealing temperatures on ductile fractures. According to these microfractographs, coarser martensite structures at higher annealing temperatures produce larger dimples on the fracture surfaces. Because the (IQ) treatment produces a finer microstructure, there is less spacing between martensite particles, thereby reducing stress concentrations. As a result, cavities begin to form later in the plastic deformation phase. Microcavities form and merge during fracture in dual-phase steel, and the well-distributed, fibrous martensite morphology at the fracture site improves ductility and elongation [35].

The fractographies of tensile fractures in (SQ) specimens of X60 (DP) steel at several intercritical

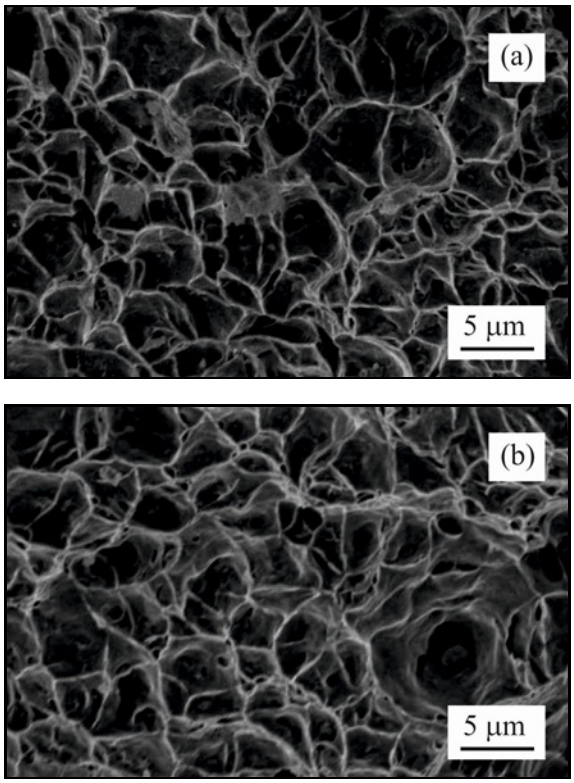

Fig. 6. Tensile fracture facies of X60 steel according to IQ treatment: (a) $T = 740\,^{\circ}\mathrm{C}$, and (b) $T = 780\,^{\circ}\mathrm{C}$.

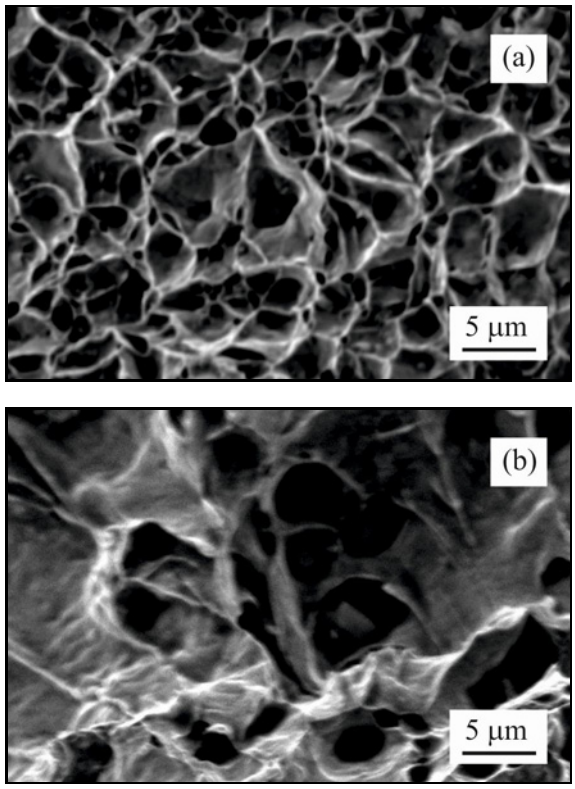

Fig. 7. Tensile fracture facies of X60 steel according to SQ treatment: (a) $T = 740\,^{\circ}\mathrm{C}$ and (b) $T = 780\,^{\circ}\mathrm{C}$.

annealing temperatures are displayed in Fig. 7. Large dimples are indicative of ductile fracture, which is more common at lower temperatures. High intercritical temperatures, on the other hand, cause a dominant brittle fracture, which is a sign of early failure during the early stages of deformation. There is a significant average distance between the martensite particles in the banded microstructure resulting from (SQ) treatment. During plastic deformation, this configuration promotes the formation of microcavities by increasing dislocation density and stress concentrations in the surrounding ferrite. In dual-phase steels treated with (SQ), cleavage crack propagation in ferrite leads to premature fractures, often with slight plastic deformation.

Furthermore, the cleavage morphologies observed in (SQ) samples are consistent with those reported for comparable steel types in the literature [36–38]. These observations support the conclusion that the ductility of the (IQ) microstructure is much higher than that of the other microstructures at the same temperature (IAT).

5. Conclusions

1. The initial microstructural state of X60 steel before reaching the intercritical range has a significant influence on the morphology and distribution of martensite. The IQ, DQ, and SQ treatments exhibit fine and fibrous martensite uniformly distributed in ferrite, dispersed martensite islands within a polygonal ferritic matrix, and a banded ferrite-martensite microstructure, respectively.

2. Generally, the best tensile properties are associated with finer microstructures in X60 steel. The distribution and dispersion of martensite islands are crucial for achieving optimal mechanical performance. The IQ treatment provided a better combination of strength and ductility.

3. The work hardening behavior of X60 steel exhibits a non-linear variation, governed by a two-stage mechanism. For all examined microstructures, the first-stage work hardening coefficient (n_1) exceeds the second-stage coefficient (n_2), and both (n_1) and (n_2) increase with higher intercritical annealing temperatures.

4. Different intercritical annealing temperatures affect the tensile fracture characteristics of IQ specimens produced from X60 steel. Elevated annealing temperatures result in larger fracture-surface dimples and coarser martensite.

5. Fractographic analysis of tensile fractures in SQ-treated X60 steel reveals that brittle fractures, indica-

tive of premature failure, are prevalent at high intercritical annealing temperatures. In contrast, ductile fractures characterized by pronounced surface dimples are more typical at lower annealing temperatures.

References

[1] A. Refaee, S. Ataya, S. Ibrahim, Effect of dual phase steel processing conditions on the microstructure and mechanical properties, J. Pet. Min. Eng. 18 (2016) 20–26. https://doi.org/10.21608/jpme.2018.37226

[2] A. Verma, R. K. Saxena, A new method to generate artificial microstructure of dual phase steel using Teacher-Learner Based Optimization, Sâdhanâ 44 (2019) 85. https://doi.org/10.1007/s12046-019-1054-8

[3] C. Liu, Y. Du, X. Wang, Z. Hu, P. Li, K. Wang, D. Liu, B. Jiang, Mechanical and tribological behavior of dual-phase ductile iron with different martensite amounts, J. Mater. Res. Technol. 24 (2023) 2978–2987. https://doi.org/10.1016/j.jmrt.2023.03.210

[4] A. Skowronek, A. Grajcar, R. H. Petrov, Dependence of mechanical properties on the phase composition of intercritically annealed medium-Mn steel as the main competitor of high-strength DP steels, Sci. Rep. 14 (2024) 9567. https://doi.org/10.1038/s41598-024-60295-0

[5] W. Dong, L. Bao, W. Li, K. Shin, C. Han, Effects of laser forming on the mechanical properties and microstructure of DP980 steel, Mater. 15 (2022) 7581. https://doi.org/10.3390/ma15217581

[6] Z.-P. Zhao, G.-Y. Qiao, L. Tang, H.-W. Zhu, B. Liao, F.-R. Xiao, Fatigue properties of X80 pipeline steels with ferrite/bainite dual-phase microstructure, Mater. Sci. Eng. A 657 (2016) 96–103. https://doi.org/10.1016/j.msea.2016.01.043

[7] P. Zhou, L. Wang, C. Cui, Effect of intercritical temperature on the microstructure and mechanical properties of 10CrMnMoSi dual-phase steel, J. Mater. Eng. Perform. 32 (2023) 8949–8960. https://doi.org/10.1007/s11665-022-07747-8

[8] X. Hao, X. Zhao, B. Huang, Influence of intercritical quenching temperature on microstructure, mechanical properties, and corrosion resistance of dual-phase steel, J. Mater. Eng. Perform. 29 (2020) 4446–4456. https://doi.org/10.1007/s11665-020-04928-1

[9] A. Pineau, A.A. Benzerga, T. Pardoen, Failure of metals I: Brittle and ductile fracture, Acta Mater. 107 (2016) 424–483. https://doi.org/10.1016/j.actamat.2015.12.034

[10] P. Shi, Y. Ren, X. Zhang, H. Wang, J. Chen, Y. Pei, J. Yan, H. Zheng, J. Zhang, Role of martensite morphology on mechanical response of dual-phase steel produced by partial reversion from martensite, Mater. Sci. Eng. A 893 (2024) 146116. https://doi.org/10.1016/j.msea.2024.146116

[11] O. R. Terrazas, K. O. Findley, C. J. Van Tyne, Influence of martensite morphology on sheared-edge formability of dual-phase steels, ISIJ Int. 57 (2017) 937–944. https://doi.org/10.2355/isijinternational.ISIJINT-2016-602

[12] O. Abedini, M. Behroozi, P. Marashi, M. Pouranvari, Intercritical heat treatment temperature dependence of mechanical properties and corrosion resistance of dual-phase steel, Mater. Res. 22 (2019). https://doi.org/10.1590/1980-5373-mr-2017-0969

[13] H. Zhang, B. Fu, N. Kang, Z. Xi, Mechanical properties and rolling-sliding wear performance of dual phase austempered ductile iron as potential metro wheel material, Wear 406–407 (2018) 98–106. https://doi.org/10.1016/j.wear.2018.04.006

[14] D. Xu, Y. Cheng, G. Yang, G. Zhao, S. Bao, The influence of annealing temperature on structure morphology and mechanical properties of prequenching-quenching and partitioning steel, Mater. 15 (2022) 4156. https://doi.org/10.3390/ma15124156

[15] E. Erişir, O. G. Bilir, Effect of intercritical annealing temperature on phase transformations in medium carbon dual phase steels, J. Mater. Eng. Perform. 23 (2014) 1055–1061. https://doi.org/10.1007/s11665-013-0848-9

[16] Y. Hu, X. Zuo, R. Li, Z. Zhang, Effect of initial microstructures on the properties of ferrite-martensite dual-phase pipeline steels with strain-based design, Mater. Res. 15 (2012) 317–322. https://doi.org/10.1590/S1516-14392012005000021

[17] L. Shi, Z. Yan, Y. Liu, C. Zhang, Z. Qiao, Improved toughness and ductility in ferrite/acicular ferrite dual-phase steel through intercritical heat treatment, Mater. Sci. Eng. A 590 (2014) 7–15. https://doi.org/10.1016/j.msea.2013.10.006

[18] E. Ahmad, T. Manzoor, M. M. A. Ziai, Effect of martensite morphology on tensile deformation of dual-phase steel, J. Mater. Eng. Perform. 21 (2011) 1–6. https://doi.org/10.1007/s11665011-9934-z

[19] B. Krebs, L. Germain, A. Hazotte, M. Goune, Banded structure in dual phase steels in relation to the austenite-to-ferrite transformation mechanisms, J. Mater. Sci. 46 (2011) 7026–7038. https://doi.org/10.1007/s10853-011-5671-9

[20] J. D. Verhoeven, A review of microsegregation induced banding phenomena in steels, J. Mater. Eng. Perform. 9 (2000) 286–296. https://doi.org/10.1361/105994900770345935

[21] S. Zidelmel, K. Rayane, A. Kaouka, Effects of thermomechanical parameters on microstructural and mechanical properties of API X70, JOM 76 (2024) 3354–3361. https://doi.org/10.1007/s11837-023-06333-0

[22] T. Mansouri, S. Zidelmel, Effect of austenitizing temperature on transformation of banded dual-phase structures, Kovove Mater. 63 (2025) 135–145. https://doi.org/10.31577/km.2025.3.135

[23] D. Avendaño-Rodríguez, J. D. Granados, E. Espejo-Mora, L. Mujica-Roncery, R. Rodríguez-Baracaldo, Fracture mechanisms in dual-phase steel: Influence of martensite volume fraction and ferrite grain size, J. Eng. Sci. Technol. Rev. 11 (2018) 174–181. https://doi.org/10.25103/jestr.116.22

[24] M. Mukherjee, S. K. Das, S. Karmakar, S. Bera, S. Kundu, Effect of martensite morphology and volume fraction on strain hardening and fracture behaviour of dual phase steel, Mater. Sci. Eng. A 707 (2017) 284–293. https://doi.org/10.1016/j.msea.2017.09.065

[25] Z. H. Cong, N. Jia, X. Sun, Stress and strain partitioning of ferrite and martensite during deformation, Metall. Mater. Trans. A 40 (2009) 1383–1387. https://doi.org/10.1007/s11661-009-9824-2
[26] S. K. Paul, Effect of martensite volume fraction on stress triaxiality and deformation behavior of dual-phase steel, Mater. Des. 50 (2013) 782–789. https://doi.org/10.1016/j.matdes.2013.03.096
[27] A. Bag, K. K. Ray, E. S. Dwarakadasa, Influence of martensite content and morphology on toughness and fatigue behavior of high-martensite dual-phase steels, Metall. Mater. Trans. A 32 (2001) 2207–2217. https://doi.org/10.1007/s11661-001-0196-5
[28] A. Bayram, A. Uguz, Effects of microstructure and notches on the mechanical properties of dual-phase steels, Mater. Charact. 43 (1999) 259–269. https://doi.org/10.1016/S1044-5803(99)00044-3
[29] M. Davari, M. Mansouri, Investigation of intercritical heat treatment temperature effect on microstructure and mechanical properties of dual phase steel, Metall. Mater. Eng. 23 (2017) 143–152. https://doi.org/10.30544/293
[30] A. Zare, A. Ekrami, Effect of martensite volume fraction on work hardening behavior of triple phase steels, Mater. Sci. Eng. A 528 (2011) 4422–4426. https://doi.org/10.1016/j.msea.2011.02.021
[31] M. S. Mohsenzadeh, Justification of changes in work hardening exponent based on micro-mechanisms of deformation in plain carbon steel, Arch. Metall. Mater. 69 (2024) 997–1003. https://doi.org/10.24425/amm.2024.150920
[32] P. Movahed, S. Kolahgar, S. P. H. Marashi, M. Pouranvari, N. Parvin, Effect of intercritical heat treatment temperature on tensile properties and work hardening behavior of ferrite–martensite dual-phase steel sheets, Mater. Sci. Eng. A 518 (2009) 1–6. https://doi.org/10.1016/j.msea.2009.05.046
[33] A. Zare, A. Ekrami, Effect of martensite volume fraction on work hardening behavior of triple phase steels, Mater. Sci. Eng. A 528 (2011) 4422–4426. https://doi.org/10.1016/j.msea.2011.02.021
[34] Y. Zhai, W. Su, F. Guo, X. Zheng, B. Yang, Q. Wang, Y. Li, W. Cao, C. Huang, Experimental and numerical investigation of yield point phenomenon and strain partitioning in dual-phase steel with lamellar structure, Mater. Sci. Eng. A 897 (2024) 146356. https://doi.org/10.1016/j.msea.2024.146356
[35] S. E. Offerman, N. H. Van Dijk, M. Th. Rekveldt, J. Sietsma, S. Van der Zwaag, Ferrite/pearlite band formation in hot-rolled medium carbon steel, Mater. Sci. Technol. 18 (2002) 297–303. https://doi.org/10.1179/026708301225000752
[36] D. Das, P. P. Chattopadhyay, Influence of martensite morphology on the work-hardening behavior of high-martensite (ferrite-martensite) dual-phase steel, J. Mater. Sci. 44 (2009) 2957–2965. https://doi.org/10.1007/s10853-009-3392-0
[37] P. Das, P. P. Chattopadhyay, N. R. Bandyopadhyay, A study on the effect of martensite morphology on mechanical properties of high-martensite dual-phase steels, J. Metall. Mater. Eng. 84 (2003) 68–79.
[38] J. Zhang, H. Di, Y. Deng, R. D. K. Misra, Effect of martensite morphology and volume fraction on strain hardening and fracture behavior of martensite-ferrite dual phase steel, Mater. Sci. Eng. A 627 (2015) 230–240. https://doi.org/10.1016/j.msea.2014.12.031